On Fast Multi-Objective Optimization of Antenna Structures Using Pareto Front Triangulation and Inverse Surrogates

Anna Pietrenko-Dabrowska[1[0000-0003-2319-6782]], Slawomir Koziel[1,2[0000-0002-9063-2647]], and Leifur Leifsson[3[0000-0001-5134-870X]]

[1] Faculty of Electronics Telecommunications and Informatics, Gdansk University of Technology, Narutowicza 11/12, 80-233 Gdansk, Poland
anna.dabrowska@pg.edu.pl
[2] Engineering Optimization & Modeling Center, School of Science and Engineering, Reykjavík University, Menntavegur 1, 101 Reykjavík, Iceland
koziel@ru.is
[3] Department of Aerospace Engineering, Iowa State University, Ames, IA 50011, USA
leifur@iastate.edu

Abstract. Design of contemporary antenna systems is a challenging endeavor, where conceptual developments and initial parametric studies, interleaved with topology evolution, are followed by a meticulous adjustment of the structure dimensions. The latter is necessary to boost the antenna performance as much as possible, and often requires handling several and often conflicting objectives, pertinent to both electrical and field properties of the structure. Unless the designer's priorities are already established, multi-objective optimization (MO) is the preferred way of yielding the most comprehensive information about the best available design trade-offs. Notwithstanding, MO of antennas has to be carried out at the level of full-wave electromagnetic (EM) simulation models which poses serious difficulties due to high computational costs of the process. Popular mitigation methods include surrogate-assisted procedures; however, rendering reliable metamodels is problematic at higher-dimensional parameter spaces. This paper proposes a simple yet efficient methodology for multi-objective design of antenna structures, which is based on sequential identification of the Pareto-optimal points using inverse surrogates, and triangulation of the already acquired Pareto front representation. The two major benefits of the presented procedure are low computational complexity, and uniformity of the produced Pareto set, as demonstrated using two microstrip structures, a wideband monopole and a planar quasi-Yagi. In both cases, ten-element Pareto sets are generated at the cost of only a few hundreds of EM analyses of the respective devices. At the same time, the savings over the state-of-the-art surrogate-based MO algorithm are as high as seventy percent.

Keywords: Antenna systems, electromagnetic simulation, design optimization, multi-objective design, inverse modeling.

ICCS Camera Ready Version 2021
To cite this paper please use the final published version:
DOI: 10.1007/978-3-030-77970-2_10

1 Introduction

Design of modern antenna structures is a complex process involving several stages that include, among others, conceptual development, topology evolution (typically supported by parametric studies), as well as design closure, i.e., the final adjustment of antenna parameters. Nowadays, antenna geometries become more and more complex in order to meet the increasing performance requirements related to particular application areas such as wireless communications [1], [2], internet of things (IoT) [2], or wearable [4], and implantable devices [5]. More often than not, design specifications include additional functionalities such as multi-band operation [6], tunability [7], or circular polarization [8]. Proper tuning of antenna dimensions is instrumental in achieving the best possible performance, yet it is challenging. For reliability reasons, it has to be carried out using full-wave electromagnetic (EM) simulation tools, which entails considerable computational expenses.

The problem is exacerbated by the necessity of handling several objectives, which are typically conflicting so that the enhancement of one leads to degradation of others. A representative example are compact antennas where reduction of physical dimensions has detrimental effects on both electrical and field properties of the structure (e.g., [9]). Consequently, practical design requires identification of the trade-off solutions. This can only be achieved using numerical optimization techniques. However, conventional algorithms, both local (gradient-based [10], pattern search [11]), and population-based metaheuristics (e.g., differential evolution [12], particle swarm optimizers [13]) are only capable of processing scalar objectives. To allow the employment of conventional methods, multi-objective problems are often reformulated, using e.g., objective aggregation [14], or objective prioritization [15]. Rendering comprehensive information about available design trade-offs requires genuine multi-objective optimization (MO) [16]. Undoubtedly, the most popular solution approaches are MO versions of population-based metaheuristic algorithms, e.g., evolutionary algorithms [17], differential evolution [18], particle swarm optimization [19], and many others [20]-[23]. The advantage of population-based methods is that the Pareto set can be generated within a single algorithm run. However, the computational cost of these algorithms is high. As a matter of fact, it is normally prohibitive when executed at the level of EM simulations.

Nature-inspired procedures can be accelerated by incorporating surrogate modelling methods [24]. Unfortunately, due to high nonlinearity of antenna characteristics, the curse of dimensionality becomes the major obstacle so that construction of reliable surrogates within the entire parameter space of interest is only possible for structures described by few parameters [25]. This can be mitigated to a certain extent using machine learning approaches, where the initial surrogate is gradually refined using additional EM data acquired with the use of appropriate infill criteria [26]. Widely used modelling techniques include kriging [27], Gaussian process regression [28], and support vector regression [29]. Another possibility has been offered by constrained modelling procedures that limit the surrogate model domain to a relevant regions of the space (e.g., those containing the Pareto front in the case of MO problems) [30], [31]. All the aforementioned techniques are stochastic. Recently, deterministic surrogate-based MO frameworks have been developed as well, including point-by-point Pareto front exploration [32], generalized bisection [33], as well as sequential domain patching (SDP) [34]. The most important advantage of deterministic algorithms is in eliminating the

ICCS Camera Ready Version 2021
To cite this paper please use the final published version:
DOI: 10.1007/978-3-030-77970-2_10

need to construct globally accurate surrogates (most operations are executed using local metamodels [35]).

This work discusses a novel deterministic surrogate-assisted framework for MO of antennas. The foundation of the presented approach is sequential generation of the Pareto-optimal designs using inverse surrogates and triangulation of the already available representation of the Pareto front. The framework is capable of handling any number of objectives, and allows for a rendition of uniformly distributed Pareto sets. Furthermore, it is computationally efficient, which is demonstrated using two antenna examples: a broadband monopole, and a planar Yagi antenna. In both cases, ten element sets of trade-off designs are obtained at the cost of only a few hundreds of EM simulations of the respective structures. It is also shown that our approach is competitive to state-of-the-art surrogate-assisted methods in terms of the CPU cost of the MO process, but also the uniformity of the obtained Pareto set.

2 Multi-Objective Design of Antenna Structures Using Inverse Surrogates and Pareto Set Triangulation

The purpose of this section is to formulate the MO procedure being the subject of this work. We discuss the basic components of the algorithm with the emphasis on the inverse surrogate modeling and Pareto set triangulation, as a way of generating the initial designs to obtain additional trade-off solutions, further tuned using the customized local refinement procedure.

2.1 Antenna Design for Multiple Performance Figures. Problem Formulation

It is assumed that the antenna structure of interest is to be designed with respect to N_{obj} figures of interest (objectives), F_k, $k = 1, \ldots, N_{obj}$, all to be minimized. Here, the MO process is understood as identification of Pareto-optimal points [36] representing the best possible trade-offs between the considered objectives. The objective vector will be denoted as $\boldsymbol{F} = [F_1\ F_2\ \ldots\ F_{Nobj}]^T$.

The antenna outputs (typically, frequency responses such as reflection coefficient, gain, etc.), are obtained by means of full-wave electromagnetic (EM) analysis. The aggregated vector of antenna characteristics is denoted as $\boldsymbol{R}(\boldsymbol{x})$, where $\boldsymbol{x}$ stands for adjustable parameters (typically, antenna dimensions). As mentioned in Section 1, direct MO of antenna structures at the level of EM analysis tends to be expensive in computational terms.

2.2 Inverse Surrogate. Triangulation of Pareto-Optimal Solution Set

We will denote by $\boldsymbol{x}^{(k)}$, $k = 1, \ldots, p$, the elements of the Pareto set identified by iteration k of the MO algorithm; $\boldsymbol{F}^{(k)} = \boldsymbol{F}(\boldsymbol{x}^{(k)}) = [F_1^{(k)}\ \ldots\ F_{Nobj}^{(k)}]^T$ stand for the corresponding objective vectors. Among them, the first N_{obj} Pareto-optimal points are obtained by solving the single-objective tasks

$$\boldsymbol{x}^{(k)} = \arg\min_{\boldsymbol{x}\in X} F_k\left(\boldsymbol{R}(\boldsymbol{x})\right) \tag{1}$$

These vectors determine the span of the Pareto front and are the basis to find the remaining solutions. The process is iterative, and involves triangulation of the existing set, as well as auxiliary inverse surrogate models.

ICCS Camera Ready Version 2021
To cite this paper please use the final published version:
DOI: 10.1007/978-3-030-77970-2_10

Consider the inverse surrogate (metamodel) $\boldsymbol{s}(\boldsymbol{F}) : F \rightarrow X$, where F and X are the objective and parameter spaces of the MO problem, respectively. The training data to render the surrogate is $\{\boldsymbol{F}^{(k)}, \boldsymbol{x}^{(k)}\}_{k=1,\ldots,p}$. Note that $\boldsymbol{s}$ is referred to as inverse because its set of values is the parameter space of the antenna at hand. In other words, the surrogate makes predictions concerning the Pareto-optimal designs corresponding to the specific objective vectors $\boldsymbol{F}$. In contrast, typically considered forward models are used to predict antenna responses corresponding to specific parameter vectors $\boldsymbol{x}$. Here, the surrogate is set up using kriging interpolation [37].

The second tool utilized in the proposed methodology is triangulation of the Pareto set $\{\boldsymbol{F}^{(k)}\}_{k=1,\ldots,p}$, the result of which is a set of simplexes $\boldsymbol{S}^{(j)}$, $j = 1, ..., K_p$. In this work, the simplexes are considered in the objective space, and represented by vertices $\boldsymbol{S}^{(j)} = \{\boldsymbol{F}^{(j.1)},\ldots,\boldsymbol{F}^{(j.Nobj)}\}$, where $\boldsymbol{F}^{(j.r)} \in \{\boldsymbol{F}^{(k)}\}_{k=1,\ldots,p}$, for $r = 1, \ldots, N_{obj}$. In order to avoid degenerate simplexes, Delaunay triangulation is employed [38].

2.3 Infill Points and Refinement Procedure

The set of simplexes $\boldsymbol{S}^{(j)}$ constructed in Section 2.2 can be considered as a partitioning of the current Pareto set. Additional Pareto-optimal points are found using a sequential sampling process as described below. Let $A(\boldsymbol{S}^{(j)})$ stand for the volume of $\boldsymbol{S}^{(j)}$, and

$$j_{\max} = \arg \max_{1 \le j \le N_{obj}} \{A(\boldsymbol{S}^{(j)})\} \tag{2}$$

be the index of the largest volume simplex. Using (2), the new objective vector $\boldsymbol{F}_{tmp}$ is established as

$$\boldsymbol{F}_{tmp} = \frac{1}{N_{obj}} \sum_{k=1}^{N_{obj}} \boldsymbol{F}^{(j_{\max}.k)} \tag{3}$$

More specifically, $\boldsymbol{F}_{tmp} = [F_{tmp.1} \ldots F_{tmp.Nobj}]^T$ is the centre of the simplex featuring the largest volume among the set $\boldsymbol{S}^{(j)}$, $j = 1, \ldots, K_p$.

At this point, the inverse surrogate $\boldsymbol{s}$ introduced in Section 2.2 is employed to find the representation $\boldsymbol{x}_{tmp}$ of $\boldsymbol{F}_{tmp}$ in the parameter space as

$$\boldsymbol{x}_{tmp} = \boldsymbol{s}(\boldsymbol{F}_{tmp}) \tag{4}$$

An alternative initial design is also produced as the centre of $\boldsymbol{S}^{(j\max)}$ in the parameter space, i.e.,

$$\boldsymbol{x}_{tmp.alt} = \frac{1}{N_{obj}} \sum_{k=1}^{N_{obj}} \boldsymbol{x}^{(j_{\max}.k)} \tag{5}$$

The vectors $\boldsymbol{x}^{(j\max.k)} \in X$, $k = 1, \ldots, N_{obj}$, correspond to $\boldsymbol{F}^{(j\max.)} \in F$. Analytically, $\boldsymbol{x}_{tmp.alt}$ is identified similarly as in (4) but using the linear model established using the (parameter space) vertices of the simplex $\boldsymbol{S}^{(j\max)}$. The 'ultimate' initial design is then selected as the better of the two, $\boldsymbol{x}_{tmp}$ and $\boldsymbol{x}_{tmp.alt}$, in terms of the smaller value of the objective F_1. The alternative vector (5) is considered because of possibly poor predictive power of the surrogate $\boldsymbol{s}$ at certain stages of the MO process, which is primarily the effect of low cardinality of the Pareto set.

The next stage of the optimization process is design refinement. It is necessary because the initial design (whether $\boldsymbol{x}_{tmp}$ or $\boldsymbol{x}_{tmp.alt}$) is only an approximation of the true Pareto optimal point, and it normally needs to be relocated towards the Pareto front. Here, it is realized by solving a local optimization task formulated as

ICCS Camera Ready Version 2021
To cite this paper please use the final published version:
DOI: 10.1007/978-3-030-77970-2_10

$$\boldsymbol{x}^{(p+1)} = \arg \min_{\substack{\boldsymbol{x},\, F_2(\boldsymbol{x}) \le F_{tmp.2} \\ \vdots \\ F_{N_{obj}}(\boldsymbol{x}) \le F_{tmp.N_{obj}}}} F_1\left(\boldsymbol{R}(\boldsymbol{x})\right) \tag{6}$$

According to (6), we aim at minimizing the first objective without degrading the remaining ones (as compared to their values $\boldsymbol{F}_{tmp}$ at the initial design). In this work, (6) is solved by means of trust-region gradient-based procedure. More specifically, a series $\boldsymbol{x}^{(p+1.i)}$, $i = 0, 1, \ldots$, of approximations to $\boldsymbol{x}^{(p+1)}$ is generated as

$$\boldsymbol{x}^{(p+1.i+1)} = \arg \min_{\substack{\boldsymbol{x},\, \boldsymbol{x}^{(p+1.i)} - \boldsymbol{d}^{(i)} \le \boldsymbol{x} \le \boldsymbol{x}^{(p+1.i)} + \boldsymbol{d}^{(i)} \\ F_2(\boldsymbol{x}) \le F_{tmp.2} \\ \vdots \\ F_{N_{obj}}(\boldsymbol{x}) \le F_{tmp.N_{obj}}}} F_1\left(\boldsymbol{L}^{(i)}(\boldsymbol{x})\right) \tag{7}$$

In (7), $\boldsymbol{L}^{(i)} = \boldsymbol{R}(\boldsymbol{x}^{(p+1.i)}) + \boldsymbol{J_R}(\boldsymbol{x}^{(p+1.i)})\cdot(\boldsymbol{x} - \boldsymbol{x}^{(p+1.i)})$ is the first-order Taylor model of $\boldsymbol{R}$ at $\boldsymbol{x}^{(p+1.i)}$, established using the Jacobian matrix $\boldsymbol{J_R}$. The latter is estimated by means of finite differentiation (for $i = 0$). Subsequently, $\boldsymbol{J_R}$ is updated using the rank-one Broyden formula [39], which is sufficient as $\boldsymbol{x}^{(p+1.0)} = \boldsymbol{x}_{tmp}$ is normally close to $\boldsymbol{x}^{(p+1)}$. Furthermore, the predictive power of the metamodel $\boldsymbol{s}$ will improve over time due to reduced distances between the Pareto-optimal vectors $\boldsymbol{x}^{(k)}$. A conceptual illustration of the MO process has been provided in Fig. 1.

Upon solving (6), the vector $\boldsymbol{x}^{(p+1)}$ complements the Pareto set, which is then used to enhance the surrogate $\boldsymbol{s}$ with the updated training data set $\{\boldsymbol{F}^{(k)}, \boldsymbol{x}^{(k)}\}_{k = 1,\ldots,p+1}$. This concludes the pth iteration of the MO procedure. The algorithm is terminated upon yielding the required number of Pareto-optimal points.

2.4 Optimization Framework

The flow diagram of the overall MO procedure has been shown in Fig. 2. As mentioned before, the first step is to acquire the extreme Pareto-optimal points $\boldsymbol{x}^{(k)}$, $k = 1, \ldots, N_{obj}$, obtained by solving the single-objective task (1) (cf. Section 2.2). This data is used to construct the metamodel $\boldsymbol{s}$. The surrogate is applied to generate the initial design $\boldsymbol{x}_{tmp}$. The latter is the image $\boldsymbol{s}(\boldsymbol{F}_{tmp})$ of the objective vector calculated as the centre of the largest simplex produced through triangulation of the Pareto set available so far in the MO process. The final stage of the algorithm iteration is design refinement (cf. (6), (7)), where the vector $\boldsymbol{x}_{tmp}$ is 'pushed' towards the Pareto front through minimization of the first objective, while imposing constraints on the remaining ones. The CPU cost of the refinement step is low because of employing sparse Jacobian updates. The termination condition is based on identification of the required number of parameter vectors.

One of the intrinsic advantages of the presented MO procedure is that it is fully deterministic. In particular, no randomized optimization techniques are involved, which also allows us to estimate the cost of the search process beforehand. The fact of utilizing the already existing knowledge about the Pareto set in the form of the inverse surrogate further improves the efficacy of the method.

Another advantage of the proposed approach is that it permits a uniform coverage of the Pareto front. The underlying assumption here is connectivity of the Pareto front (i.e., that it does not contain several disjoint regions or subsets). While such an assumption does not hold in general, it is normally the case for many practical antenna design tasks. The latter is mainly ensured by a continuous dependence between the antenna geometry parameters and the frequency characteristics of the structure.

ICCS Camera Ready Version 2021
To cite this paper please use the final published version:
DOI: 10.1007/978-3-030-77970-2_10

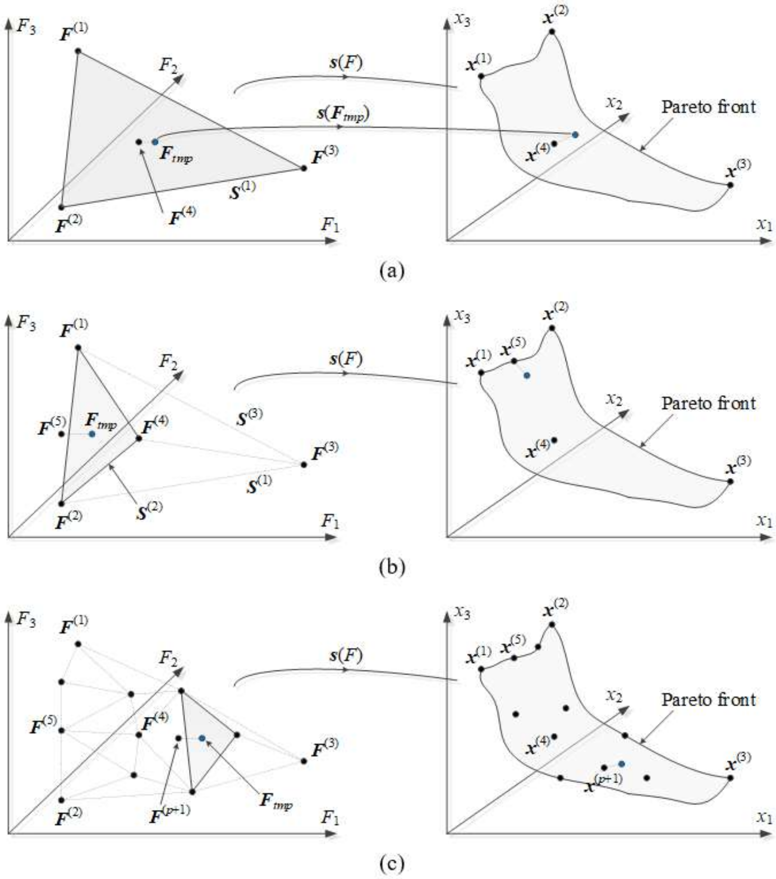

Fig. 1. Multi-objective optimization of antennas using Pareto front triangulation and inverse surrogates. The left and the right panels show the objective and the parameter spaces, respectively: (a) first iteration: the extreme Pareto-optimal designs $\boldsymbol{F}_k$, k = 1, 2, 3, are triangulated in the objective space to produce the initial point $\boldsymbol{s}(\boldsymbol{F}_{tmp})$; this design is refined (cf. (5), (6)) to obtain the new Pareto-optimal point $\boldsymbol{x}^{(4)}$ and its representation in the objective space $\boldsymbol{F}^{(4)}$; (b) second iteration of the algorithm, where the initial (objective space) design $\boldsymbol{F}_{tmp}$ is allocated in the centre of the largest simplex (here, $\boldsymbol{S}^{(2)}$); (c) one of the further iterations of the procedure.

3 Demonstration Examples

This section demonstrates the MO procedure introduced in Section 2 using two examples of microstrip antennas: a broadband monopole and a planar Yagi. Both structures are optimized with respect to two objectives each: size reduction and matching improvement (monopole), as well as matching improvement and in-band gain enhancement (Yagi). Benchmarking with respect to state-of-the-art surrogate-assisted MO algorithm is also provided.

ICCS Camera Ready Version 2021
To cite this paper please use the final published version:
DOI: 10.1007/978-3-030-77970-2_10

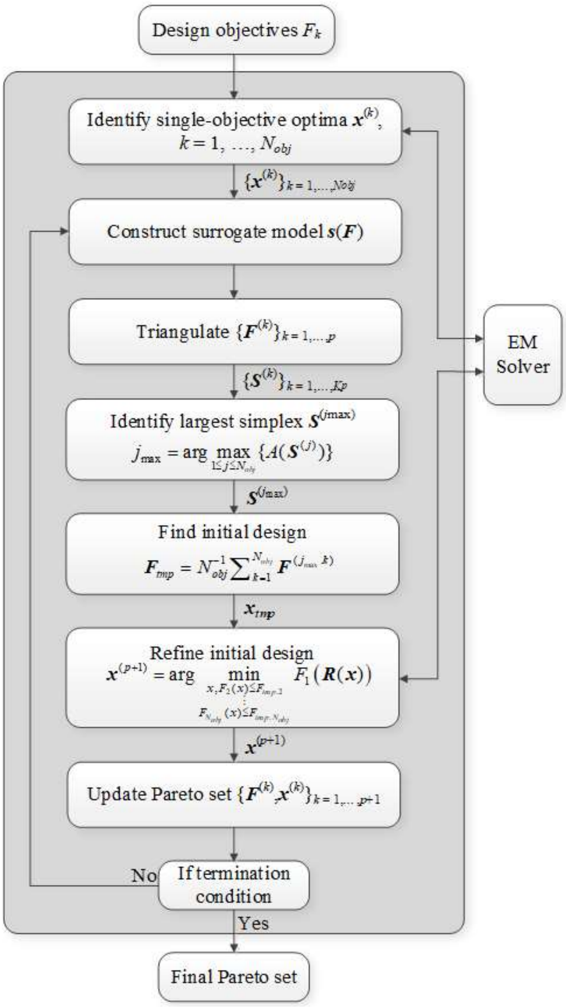

Fig. 2. Flow diagram of the proposed MO framework.

3.1 Case I: Broadband Monopole Antenna

Consider an ultra-wideband (UWB) monopole antenna [40]. The structure, shown in Fig. 3, is implemented on FR4 substrate ($\varepsilon_r = 4.3$, $h = 1.55$ mm) and described by eleven independent parameters $\boldsymbol{x} = [L_g\ L_0\ L_s\ W_s\ d\ dL\ d_s\ dW_s\ dW\ a\ b]^T$; $W_0 = 2.0$ mm is fixed to ensure 50 ohm input impedance. All parameters are in millimetres. The computational model is evaluated in CST Microwave Studio (~600,000 mesh cells, simulation time 3 minutes), and contains the SMA connector.

The monopole antenna is optimized with respect to two objectives: minimization of the maximum in-band reflection (F_1), and minimization of antenna footprint $A(\boldsymbol{x})$ (F_2). The frequency range of interest is 3.1 GHz to 10.6 GHz, whereas the size is defined as the area of the substrate $A(\boldsymbol{x}) = (a + 2o)(l_0 + l_1 + w_1)$. Furthermore, the only part of the Pareto front that is of interest consists of the designs for which $F_1 \leq -10$ dB, which is the standard acceptance level when considering antenna impedance matching.

The MO process has been conducted as described in Section 2. In the first step, the two single-objective optima have been found using the gradient-based algorithm [41]: $\boldsymbol{x}^{(1)} = [9.07\ 13.39\ 9.93\ 0.43\ 2.03\ 9.17\ 0.80\ 2.29\ 3.02\ 0.29\ 0.59]^T$ mm, $\boldsymbol{x}^{(2)} = [9.81\ 13.26\ 7.82\ 0.23\ 4.36\ 0.00\ 0.97\ 1.20\ 0.00\ 0.80\ 0.62]^T$ mm. Subsequently, eight more designs have been identified, leading to the Pareto set shown in Fig. 4 (see also Fig. 5 for antenna reflection responses at the selected designs). The breakdown of the CPU cost of the MO process can be found in Table 1. The overall expenses amount to 575 full-wave antenna simulations, which includes 403 EM analyses to find the designs $\boldsymbol{x}^{(1)}$ and $\boldsymbol{x}^{(2)}$. The average cost is 20 analyses per design (excluding extreme Pareto-optimal point generation).

Benchmarking was carried out using the surrogate-based procedure [40], which employs the kriging surrogate rendered in the interval $[\boldsymbol{l}^*\ \boldsymbol{u}^*]$ with $\boldsymbol{l}^* = \min\{\boldsymbol{x}^{(1)}, \boldsymbol{x}^{(2)}\}$ and $\boldsymbol{u}^* = \max\{\boldsymbol{x}^{(1)}, \boldsymbol{x}^{(2)}\}$; the initial Pareto set is obtained by optimizing the metamodel using a multi-objective evolutionary algorithm (MOEA) [42]. The final designs are produced using output space mapping [43].

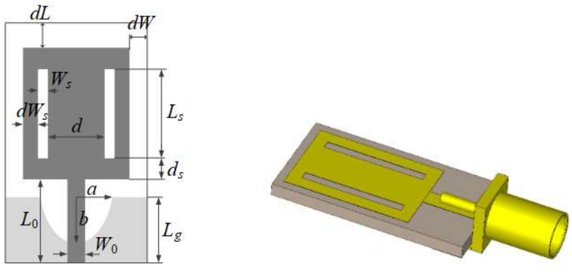

Fig. 3. Verification case I: broadband monopole antenna [40]: (a) antenna geometry (ground plane marked using the light-grey shade), (b) perspective view including the SMA connector.

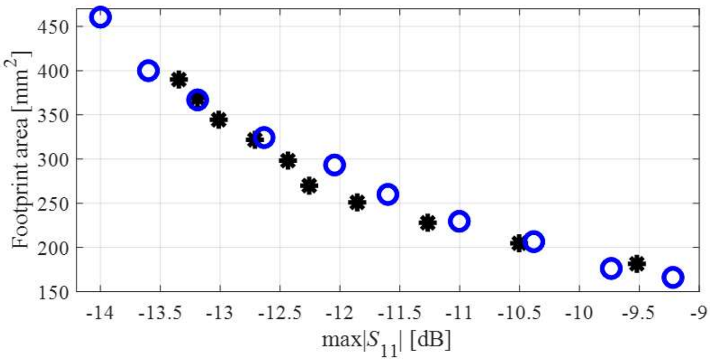

Fig. 4. Verification case I: Pareto set found by means of the proposed MO algorithm (o), the set identified using the surrogate-assisted technique of [24] (*).

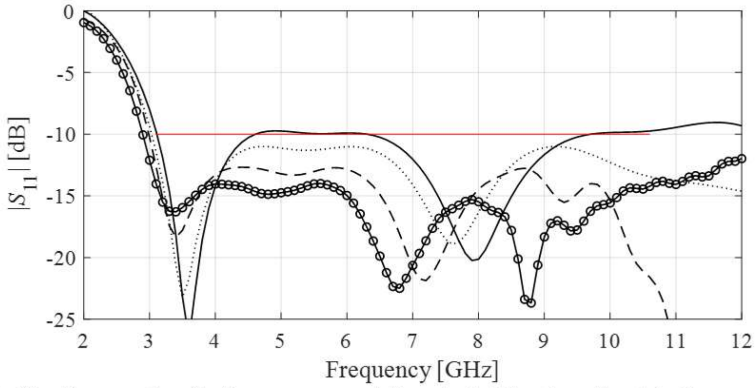

Fig. 5. Verification case I: reflection responses at the selected Pareto-optimal designs.

Table 1. Verification case I: optimization cost

This work (inverse modeling & refinement)		Surrogate-assisted procedure [24] (benchmark)	
Cost item	Cost#	Cost item	Cost#
Single-objective optimization runs (designs $\boldsymbol{x}^{(1)}$ and $\boldsymbol{x}^{(2)}$)	403 × ***R***	Single-objective optimization runs (designs $\boldsymbol{x}^{(1)}$ and $\boldsymbol{x}^{(2)}$)	403 × ***R***
		Data acquisition for kriging surrogate	1000 × ***R***
Design refinement	162 × ***R***	MOEA optimization*	N/A
		Design refinement	30 × ***R***
Total cost#	575 × ***R*** (29 h)	Total cost#	1433 × ***R*** (72 h)

* The cost of MOEA optimization is negligible compared to other stages of the process.
# The cost is expressed in terms of the equivalent number of EM simulations (marked as × ***R***).

According to the methodology of [24], restricting the domain of the surrogate to $[\boldsymbol{l}^* \ \boldsymbol{u}^*]$ allows for mitigating the problem of dimensionality to some extent. Notwithstanding, the computational cost of the benchmark algorithm is as high as 1433 EM simulations, two thirds of which are related to training data acquisition (1000 samples). This was necessary to ensure sufficient accuracy of the metamodel (7.7 percent of the average RMS error). Based on this data, it can be observed that the proposed methodology allows for sixty percent computational savings. Additionally, our approach leads to a fairly uniform coverage of the Pareto front, as well as broader span of the Pareto set as compared to the benchmark.

3.2 Case II: Planar Yagi Antenna

Consider the planar Yagi antenna [44] shown in Fig. 6. The structure is implemented on RT6010 substrate (ε_r = 10.2, h = 0.635 mm), and described by eight independent parameters $\boldsymbol{x} = [s_1\ s_2\ v_1\ v_2\ u_1\ u_2\ u_3\ u_4]^T$. The fixed parameters are $w_1 = w_3 = w_4 = 0.6$, $w_2 = 1.2$, $u_5 = 1.5$, $s_3 = 3.0$, and $v_3 = 17.5$ (dimensions in mm). Similarly as in the previous

ICCS Camera Ready Version 2021
To cite this paper please use the final published version:
DOI: 10.1007/978-3-030-77970-2_10

example, the computational model is implemented in CST Microwave Studio and evaluated using its time domain solver (~600,000 mesh cells, simulation time 4 minutes).

The intended operating frequency range of the antenna is 10 GHz to 11 GHz. The structure is optimized with respect to the following two objectives: minimization of the in-band reflection (F_1), and maximization of the average end-fire gain (F_2). The designs $\boldsymbol{x}^{(1)} = [4.38\ 3.56\ 8.90\ 4.16\ 4.08\ 4.74\ 2.15\ 1.50]^T$, and $\boldsymbol{x}^{(2)} = [5.19\ 6.90\ 7.10\ 5.08\ 3.54\ 4.78\ 2.23\ 0.93]^T$ have been found using the gradient-based search procedure [41].

The results have been shown in Figures 7 and 8, as well as Table 2. The overall cost of the MO process is 290 EM simulations of the antenna at hand, which includes 160 analyses required for rendering the designs $\boldsymbol{x}^{(1)}$ and $\boldsymbol{x}^{(2)}$. The surrogate-assisted procedure [24] has been used for the sake of comparison. The cost of the benchmark procedure is 1190 EM simulations, 1000 of which were used to construct the kriging surrogate (the average RMS error of the metamodel is 3.8 and 3.6 percent for the antenna reflection and gain, respectively). Consequently, the proposed methodology yields almost seventy percent computational savings. It can be observed that the results are consistent with those obtained in Section 3.1: our approach allows for generating a uniform coverage of the Pareto front, and with a larger span than for the benchmark.

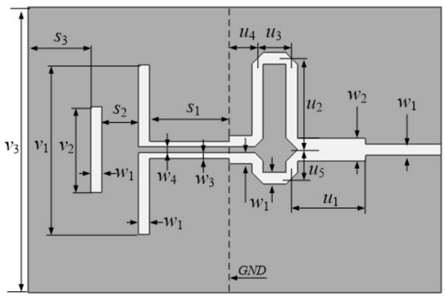

Fig. 6. Verification case II: planar Yagi antenna [44].

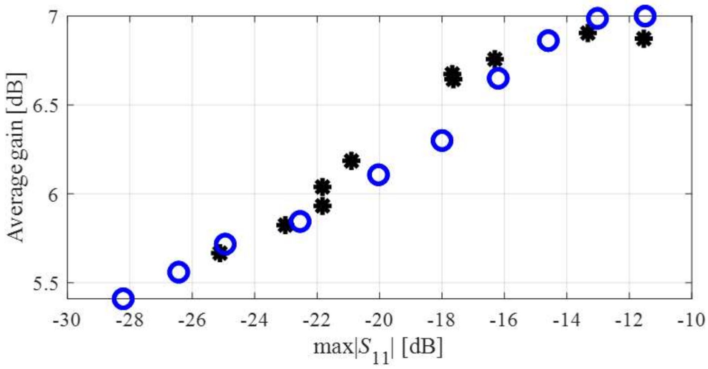

Fig. 7. Verification case II: Pareto set found using the proposed MO approach (o), the set identified using the surrogate-assisted technique of [24] (*).

ICCS Camera Ready Version 2021
To cite this paper please use the final published version:
DOI: 10.1007/978-3-030-77970-2_10

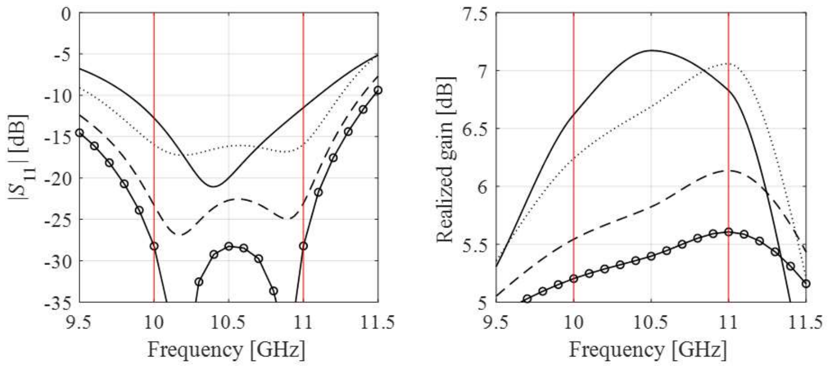

Fig. 8. Verification case II: reflection (left) and end-fire gain (right) responses for the selected Pareto-optimal designs.

Table 2. Verification case II: optimization cost

This work (inverse modeling & refinement)		Surrogate-assisted procedure [24] (benchmark)	
Cost item	Cost#	Cost item	Cost#
Single-objective optimization runs (designs $\boldsymbol{x}^{(1)}$ and $\boldsymbol{x}^{(2)}$)	160 × $\boldsymbol{R}$	Single-objective optimization runs (designs $\boldsymbol{x}^{(1)}$ and $\boldsymbol{x}^{(2)}$)	160 × $\boldsymbol{R}$
		Data acquisition for kriging surrogate	1000 × $\boldsymbol{R}$
Design refinement	130 × $\boldsymbol{R}$	MOEA optimization*	N/A
		Design refinement	30 × $\boldsymbol{R}$
Total cost#	290 × $\boldsymbol{R}$ (19.5 h)	Total cost#	1190 × $\boldsymbol{R}$ (80 h)

* The cost of MOEA optimization is negligible compared to other stages of the process.
# The cost is expressed in terms of the equivalent number of EM simulations (marked as × $\boldsymbol{R}$).

4 Conclusions

In the paper, a deterministic framework for multi-objective design of antenna structures has been proposed. The foundation of our technique is a sequential generation of the Pareto set elements using triangulation of already rendered points, as well as the inverse surrogates. A local gradient-based refinement is also involved to improve the design quality. The major benefits of the presented approach include no need to engage stochastic search procedures (in particular, population-based metaheuristics), low computational cost, and uniform coverage of the Pareto front. These features have been corroborated using two examples of microstrip antennas optimized for matching improvement, reduction of the footprint area, and maximization of the in-band gain. In both cases, ten-element Pareto sets have been obtained at the cost of a few hundreds of EM analysis of the respective structures, which yields about seventy percent savings as compared to the state-of-the-art surrogate-based technique. The proposed framework can be considered an alternative to available techniques for efficient and reliable MO of antennas, especially when handling miniaturized structures, where one of the objectives is a reduction of the physical dimensions of the radiator.

Acknowledgement

The authors would like to thank Dassault Systemes, France, for making CST Microwave Studio available. This work is partially supported by the Icelandic Centre for Research (RANNIS) Grant 206606051 and by National Science Centre of Poland Grant 2018/31/B/ST7/02369.

References

1. Ren, Z., Zhao, A., Wu, S.: MIMO antenna with compact decoupled antenna pairs for 5G mobile terminals. IEEE Ant. Wireless Prop. Lett. **18**(7), 1367–1371 (2019)
2. Zhao, A., Ren, Z.: Size reduction of self-isolated MIMO antenna system for 5G mobile phone applications. IEEE Ant. Wireless Prop. Lett. **18**(1), 152–156 (2019)
3. Houret, T., Lizzi, L., Ferrero, F., Danchesi, C., Boudaud, S.: DTC-enabled frequency-tunable inverted-F antenna for IoT applications. IEEE Ant. Wireless Prop. Lett. **19**(2), 307–311 (2020)
4. Gao, G., Yang¸ C., Hu, B., Zhang, R., Wang, S.: A wide-bandwidth wearable all-textile PIFA with dual resonance modes for 5 GHz WLAN applications. IEEE Trans. Ant. Prop. **67**(6), 4206–4211 (2019)
5. Wang, J., Leach, M., Lim, E.G., Wang, Z., Pei. R., Huang. Y.: An implantable and conformal antenna for wireless capsule endoscopy. IEEE Ant. Wireless Prop. Lett. **17**(7), 1153–1157 (2018)
6. Yang, G., Zhang, S., Li, J., Zhang, Y., Pedersen, G.F.: A multi-band magneto-electric dipole antenna with wide beam-width. IEEE Access. **8**, 68820–68827 (2020)
7. Tan, L., Wu, R., Poo, Y.: Magnetically reconfigurable SIW antenna with tunable frequencies and polarizations. IEEE Trans. Ant. Prop. **63**(6), 2772–2776 (2015)
8. Kaddour, A., Bories, S., Bellion, A., Delaveaud, C.: 3-D-printed compact wideband magnetoelectric dipoles with circular polarization. IEEE Ant. Wireless Prop. Lett. **17**(11), 2026–2030 (2018)
9. Koziel, S., Cheng, Q.S., Li, S.: Optimization-driven antenna design framework with multiple performance constraints. Int. J. RF Microwave CAE. **28**(4) (2018)
10. Koziel, S., Pietrenko-Dabrowska, A.: Expedited feature-based quasi-global optimization of multi-band antennas with Jacobian variability tracking. IEEE Access. **8**, 83907–83915 (2020)
11. Kolda, T.G., Lewis, R.M., Torczon, V.: Optimization by direct search: new perspectives on some classical and modern methods. SIAM Rev. **45**, 385–482 (2003)
12. Zhao, W.J., Liu, E.X., Wang, B., Gao, S.P., Png, C.E.: Differential evolutionary optimization of an equivalent dipole model for electromagnetic emission analysis. IEEE Trans. Electromagnetic Comp. **60**(6), 1635–1639 (2018)

ICCS Camera Ready Version 2021
To cite this paper please use the final published version:
DOI: 10.1007/978-3-030-77970-2_10

13. Lalbakhsh, A., Afzal, M.U., Esselle, K.P.: Multiobjective particle swarm optimization to design a time-delay equalizer metasurface for an electromagnetic band-gap resonator antenna. IEEE Ant. Wireless Prop. Lett. **16**, 915–915 (2017)
14. Marler, R.T., Arora, J.S.: The weighted sum method for multi-objective optimization: new insights. Structural Multidisc. Opt. **41**, 853–862 (2010)
15. Ullah, U., Koziel, S., Mabrouk, I.B.: Rapid re-design and bandwidth/size trade-offs for compact wideband circular polarization antennas using inverse surrogates and fast EM-based parameter tuning. IEEE Trans. Ant. Prop. **68**(1), 81–89 (2019)
16. Mirjalili, S., Dong, J.S.: Multi-objective optimization using artificial intelligence techniques. Springer Briefs in Applied Sciences and Technology, New York (2019)
17. Carvalho, R., Saldanha, R.R., Gomes, B.N., Lisboa, A.C., Martins, A.X.: A multi objective evolutionary algorithm based on decomposition for optimal design of Yagi-Uda antennas. IEEE Trans. Magn. **48**(2), 803–806 (2012)
18. Goudos, S.K., Gotsis, K.A., Siakavara, K., Vafiadis, E.E., Sahalos, J.N.: A multi-objective approach to subarrayed linear antenna design based on memetic differential evolution. IEEE Trans. Ant. Prop. **61**(6), 3042–3052 (2013)
19. Zhang, Y., Liu, X., Bao, F., Chi, J., Zhang, C., Liu., P.: Particle swarm optimization with adaptive learning strategy. Knowledge-Based Syst. **196**, art. no, 105789 (2020)
20. Maddio, S., Pelosi, G., Righini, M., Selleri, S.: A multi-objective invasive weed optimization for broad band sequential rotation networks. IEEE Int. Symp. Ant. Prop., Boston, MA, 955–956 (2018)
21. Zhu, D. Z., Werner, P. L., Werner, D. H.: Multi-objective lazy ant colony optimization for frequency selective surface design. IEEE Int. Symp. Ant. Prop., Boston, MA, 2035–2036 (2018)
22. Ranjan¸ P., Mahto, S. K., Choubey., A.: BWDO algorithm and its application in antenna array and pixelated metasurface synthesis. IET Microwaves Ant. Prop. **13**(9), 1263–1270 (2019)
23. Zhang, C., Fu, X., Peng, S., Wang, Y., Chang, J.: New multi-objective optimisation algorithm for uniformly excited aperiodic array synthesis. IET Microwaves Ant. Prop. **13**(2), 171–177 (2019)
24. Koziel, S., Bekasiewicz, A.: Multi-objective design of antennas using surrogate models. World Scientific, Singapore (2016)
25. De Villiers, D.I.L., Couckuyt, I., Dhaene, T.: Multi-objective optimization of reflector antennas using kriging and probability of improvement. Int. Symp. Ant. Prop., San Diego, USA, 985–986 (2017)
26. Xiao, S., Liu, G.Q., Zhang, K.L., Jing, Y.Z., Duan, J.H., Di Barba, P., Sykulski, J.K.: Multi-objective Pareto optimization of electromagnetic devices exploiting kriging with Lipschitzian optimized expected improvement. IEEE Trans. Magn. **54**(3), paper ID 7001704 (2018)
27. Xia, B., Ren, Z., Koh, C. S.: Utilizing kriging surrogate models for multi-objective robust optimization of electromagnetic devices. IEEE Trans. Magn. **50**(2), paper 7017104 (2014)
28. Jacobs, J.P.: Characterization by Gaussian processes of finite substrate size effects on gain patterns of microstrip antennas. IET Microwaves Ant. Prop. **10**(11), 1189–1195 (2016)
29. Lv, Z., Wang, L., Han, Z., Zhao, J., Wang, W.: Surrogate-assisted particle swarm optimization algorithm with Pareto active learning for expensive multi-objective optimization. IEEE J. Automatica Sinica. **6**(3), 838–849 (2019)

ICCS Camera Ready Version 2021
To cite this paper please use the final published version:
DOI: 10.1007/978-3-030-77970-2_10

30. Koziel, S., Sigurdsson, A.T.: Multi-fidelity EM simulations and constrained surrogate modeling for low-cost multi-objective design optimization of antennas. IET Microwaves Ant. Prop. **12**(13), 2025–2029 (2018)
31. Koziel, S., Pietrenko-Dabrowska, A.: Rapid multi-objective optimization of antennas using nested kriging surrogates and single-fidelity EM simulation models. Eng. Comp. **37**(4), 1491–1512 (2019)
32. Koziel, S., Kurgan, P.: Rapid multi-objective design of integrated on-chip inductors by means of Pareto front exploration and design extrapolation. Int. J. Electromagnetic Waves Appl. **33**(11), 1416–1426, (2019)
33. Unnsteinsson, S.D., Koziel, S.: Generalized Pareto ranking bisection for computationally feasible multi-objective antenna optimization. Int. J. RF & Microwave CAE. **28**(8) (2018)
34. Amrit, A., Leifsson, L., Koziel, S.: Fast multi-objective aerodynamic optimization using sequential domain patching and multi-fidelity models. Journal of Aircraft (2020)
35. Liu, Y., Cheng, Q.S., Koziel, S.: A generalized SDP multi-objective optimization method for EM-based microwave device design. Sensors. **19**(14) (2019)
36. Deb, K.: Multi-objective optimization using evolutionary algorithms. Wiley, New York, (2001)
37. Forrester, A.I.J., Keane, A.J.: Recent advances in surrogate-based optimization. Prog. Aerospace Sci. **45**, 50–79 (2009)
38. Borouchaki, H., George, P.L., Lo, S.H.: Optimal Delaunay point insertion. Int. J. Numerical Methods in Engineering. **39**(20), 3407–3437 (1996)
39. Broyden, C.G.: A class of methods for solving nonlinear simultaneous equations. Math. Comp. **19**, 577–593 (1965)
40. Haq, M.A., Koziel, S.: Simulation-based optimization for rigorous assessment of ground plane modifications in compact UWB antenna design. Int. J. RF Microwave CAE **28**(4), e21204 (2018)
41. Conn, A.R., Gould, N.I.M., Toint, P.L.: Trust Region Methods. MPS-SIAM Series on Optimization (2000)
42. Fonseca, C.M.: Multiobjective genetic algorithms with application to control engineering problems. PhD thesis, Department of Automatic Control and Systems Engineering, University of Sheffield, Sheffield, UK (1995)
43. Koziel, S., Cheng, Q.S., Bandler, J.W.: Space mapping. IEEE Microwave Magazine. **9**(6), 105–122 (2008).
44. Kaneda, N., Deal, W.R., Qian, Y., Waterhouse, R., Itoh, T.: A broad-band planar quasi Yagi antenna. IEEE Trans. Antennas Propag. **50**, 1158–1160 (2002)

ICCS Camera Ready Version 2021
To cite this paper please use the final published version:
DOI: 10.1007/978-3-030-77970-2_10